KIF15 Accelerated The Progression of Nasopharyngeal Carcinoma and Predict Poor Prognosis

Yongli Wang (wylll@sina.com.cn)
Guangxi Medical University https://orcid.org/0000-0001-8635-9492
Yong Yang
Guangxi Medical University
Ying Qin
People's Hospital of Guangxi Zhuang Autonomous Region
Fei Liu
People's Hospital of Guangxi Zhuang Autonomous Region
Jingcheng Shu
People's Hospital of Guangxi Zhuang Autonomous Region
Bing Li
People's Hospital of Guangxi Zhuang Autonomous Region
Guangwu Huang
Guangxi Medical University
Shenhong Qu
People's Hospital of Guangxi Zhuang Autonomous Region

Research Article

Keywords: Nasopharyngeal carcinoma, KIF15, Cell apoptotic, Cell proliferation

Posted Date: April 7th, 2021

DOI: https://doi.org/10.21203/rs.3.rs-260874/v1

Abstract

Background: Nasopharyngeal carcinoma (NPC) is a common tumor in head and neck and is prevailing in China. Although treatment methods continue to improve, the prognosis of advanced patients is still unsatisfactory. Kinesin family member 15 (KIF15) is a kind of protein, which regulates the process of cell mitosis and plays an important role in several types of human cancers. This study aims to investigate the role of KIF15 in NPC.

Methods: First, the differential expression of KIF15 in NPC and para-carcinoma tissues was evaluated based on both data collected from Gene Expression Omnibus (GEO) database and immunohistochemical analysis on clinical specimens collected from in-house cohort. Next, cell lines C666-1 and CNE-2Z were selected for the construction of KIF15-knockdown cell models. Then, 3-(4,5-Dimethylthiazol-2-yl)-2,5-diphenyltetrazolium bromide (MTT) assay, flow cytometry, wound healing, Transwell and clone formation assays were used to detect the proliferation, apoptosis, migration, invasion and colony formation of nasopharyngeal carcinoma cells *in vitro*. A mouse xenograft model was constructed for *in vivo* study. Furthermore, Human Apoptosis Antibody Array kit was used to screen possible targets of KIF15 in NPC. In the end, the potential molecular mechanisms underlying the effects of KIF15 was explored through western blot analysis.

Results: The results showed that the expression of KIF15 in NPC tissues is higher than that in para-carcinoma tissues, and high levels of KIF15 expression are associated with low survival rates. In addition, knockdown of KIF15 inhibited cell proliferation, migration, invasion and colony formation ability, and promoted cell apoptosis. What's more, *in vivo* xenograft experiments showed that down-regulation of KIF15 can inhibit NPC tumor growth. Moreover, the mechanism study demonstrated a variety of apoptosis-related proteins as well as PI3K/AKT and MAPK signaling pathways may be involved in KIF15-induced regulation of NPC.

Conclusions: In short, we demonstrated that KIF15 is overexpressed and accelerated the progression of nasopharyngeal carcinoma. It can be used as a new prognostic indicator as well as a potential drug target for the treatment of NPC.

Background

Nasopharyngeal carcinoma (NPC) is a common tumor in head and neck and is prevailing in China, especially in southern regions, and most of its pathological types are undifferentiated or poorly differentiated squamous cell carcinoma. At present, studies have shown that the pathogenesis of nasopharyngeal carcinoma is closely related to genetic factors, Epstein-Barr virus (EBV) infection and regional environment [1]. Because of the occult incidence of nasopharyngeal carcinoma and the obvious tendency of local lymph node invasion and distant metastasis, about 60 ~ 70% of nasopharyngeal carcinoma patients were diagnosed when tumors with advanced stage. For these patients, combination of radiotherapy and chemotherapy have been proved to be the most efficient treatment[2]. However, about

20 ~ 30% of advanced nasopharyngeal carcinoma patients still have local recurrence or distant metastasis even after receiving standardized treatment[3]. Therefore, it is urgent to recognize the molecular mechanism involved in NPC to explore and develop more efficient therapies for NPC.

As we know, the growth and metastasis of cancer cells depend on cell mitosis and proliferation, in which cytoskeletal proteins play a key regulatory role [4]. The cytoskeletal protein system is involved in almost all life activities of cancer cells, which can maintain cancer cell morphology, participate in gene translation and protein transport, tumor signal transduction and so on[5]. Kinesin superfamily proteins (KIFs) were first found in the axons of squid nerve cells, which are considered to be an important part of the cytoskeletal protein system. They are a kind of proteins that can use the energy generated from ATP hydrolysis to produce thrust, intracellular transport or promote cell movement. Based on structural, functional and phylogenetic analyses, KIFs are classified into 14 groups. The kinesin family member 15 (KIF15) belongs to the kinesin-12 superfamily, also known as the hklp2, which is a tetramer spindle motor[6].

Accumulating evidence showed that KIF15 participates in and promotes the occurrence and development of malignant tumors. In 2014, it was demonstrated that KIF15 is overexpressed in breast cancer tissues, and is correlates with poor recurrence-free survival of Estrogen receptor (ER)-positive breast cancer patients [7]. Gao's study not only presented similar results [8], but also found that KIF15 contributes to cell proliferation and migration of breast cancer, which suggested that KIF15 is a potential oncogene in human breast cancer. Moreover, Wang *et al*. [9] found that KIF15 can promote pancreatic cancer development. Studies concerning other types of malignant tumors such as hepatocellular carcinoma [10, 11], lung adenocarcinoma [12], gastric cancer [13] and malignant peripheral nerve sheath tumors [14] also confirmed the important role of KIF15 in tumor development.

To the best of our knowledge, the role of KIF15 in NPC pathogenesis has not been investigated. As NPC is a highly aggressive type of tumor, we wondered whether KIF15 is important to NPC development. Therefore, we applied several *in vitro* and *in vivo* functional assays to explore its role in NPC and identified it as a potential therapeutic target for NPC treatment.

Methods

Bioinformatics of KIF15 expression in NPC from public database.

Gene Expression Omnibus (GEO) database was utilized to collect the expression of KIF15 in normal tissues and NPC tissues. The datasets included in this study were GSE12452 (https://www.ncbi.nlm.nih.gov/geo/query/acc.cgi?acc=GSE12452) and GSE34573(https://www.ncbi.nlm.nih.gov/geo/query/acc.cgi?acc=GSE34573), and the expression profiles were tested using the Affymetrix human genome U133 Plus2.0 array platform. We used the "Limma" package in the R statistics to screen the differentially expressed genes between NPC tissue and normal nasopharyngeal tissue samples. In all, 61 samples were included in these 2 chips. We selected 14 normal nasopharyngeal tissue samples and 47 nasopharyngeal carcinoma samples for downstream

analysis. In the process of chip information analysis, quality of the original data of the chip was first evaluated; then, data filtering and analysis were performed on the qualified data. All the probes whose signal average is less than 0.005 were filtered out. Meanwhile, in order to avoid false positive results, the differential gene expression profile screened by |Fold Change|≥1.3 and $P < 0.05$ was used to perform hierarchical cluster analysis. Follow-up analysis was performed on the data that meets the filtering criteria, including significant difference analysis and functional analysis of differential expressed genes.

Collection of clinical samples

The formalin-fixed, paraffin-embedded tissue microarray including 132 NPC tissue samples and 15 para-carcinoma tissue samples collected from 132 patients were provided by Shanghai Xinchao Biotech Company (Cat.No. HNasN132Su01). The tissue microarray protocol was approved by the Human Ethics Committee of the Taizhou Hospital of Zhejiang province. The written informed consents were collected from all patients. All tissue specimens were evaluated by pathologists, and the clinical stage was defined according to the American Joint Committee on Cancer (AJCC) (7th edition, 2010). The case collection was from January 2010 to October 2011, all patients were received concurrent chemoradiotherapy and followed up for more than 5 years, except for those who died.

Cell lines and cell culture

The human NPC cell lines (CNE-2Z, HONE-1) were obtained from Institute of cancer, Central South University. We are very grateful to Professor Sai-Wah Tsao from University of Hong Kong for generously presenting the NPC cell line C666-1, Professor Musheng Zeng from Sun Yat-Sen University for kindly providing 5-8F. In the humidified atmosphere containing 5% CO_2 at 37°C, cells were propagated in Dulbecco's Modified Eagle Medium (DMEM; Gibco, Rockville, MD), with 1% penicillin/streptavidin (Gibco) and 10% Foetal Bovine Serum (FBS, Gibco). Cell culture media was replaced every 72 h.

RNA preparation, reverse transcription and quantitative real-time PCR (qRT-PCR)

Total RNA was extracted using Trizol reagent (Sigma, Cat. No: T9424-100m). The cDNA was then synthesized using a Reverse Transcription Kit (Vazyme, Cat. No: R123-01) following the manufacturer's protocol. Real-time PCR analysis was performed using AceQ qPCR SYBR Greenmaster mix (Vazyme) on an ABI VII7 System. The $2^{-\Delta\Delta Cq}$ method was utilized for the quantification of gene expression, glyceraldehyde-3 phosphate dehydrogenase (GAPDH) served as a reference control. The following PCR primers were used: KIF15 forward, 5'-CTC TCA CAG TTG AAT GTC CTT G-3' and reverse, 5'-CTC CTT GTC AGC AGA ATG AAG-3'; GAPDH forward, 5'- TGA CTT CAA CAG CGA CAC CA -3' and reverse, 5'- CAC CCT GTT GCT GTA GCC AAA -3'. The PCR protocol was: 1 min at 95˚C; 10 sec at 95˚C, 30 sec at 60˚C for 45 cycles; 15 sec at 95˚C, 1 min at 55˚C and 15 sec at 95˚C. PCR products were separated on a 20 g/L agarose gel stained with ethidium bromide and viewed under ultraviolet light.

Nasopharyngeal carcinoma tissue microarray and immunohistochemistry

NPC tissue microarray was used for the immunostaining analysis of KIF15 protein expression. The immunohistochemical staining for the tissue microarray slide was carried out in accordance with the instructions. The samples were incubated with the rabbit anti-KIF15 antibody (1:200, cat. no. Fnab04551, fine test), and goat anti rabbit IgG H&L horseradish peroxidase (HRP) -conjugated was used as secondary antibody (1:400; cat. no. Ab97080; Abcam). Ki-67 antibody (1:300; cat. no. Ab16667; Abcam) was used in the immunohistochemistry analysis of tumor sections removed from mice models. Images were captured by a light microscope (Olympus IX73). A score was assessed according to the staining intensity and percentage of positive cells. The scores were calculated as the sum of intensity scores(0–3) and percentage scores(0–4), and a final score > 3 was considered as high expression of KIF15, while a final score ≤ 3 was considered as low expression of KIF15.

Western blot analysis

In order to determine the expression level of KIF15 in NPC cell lines, cells were collected and lysed by lysis buffer according to the manufacturer's instructions. The concentration of protein was determined using the BCA Protein Assay kit (cat. no. 23225; HyClone-Pierce). Total cellular proteins were subjected to sodium dodecyl sulfate polyacrylamide gel electrophoresis (SDS-PAGE) and then transferred to a polyvinylidene difluoride (PVDF) membrane. Membranes were then incubated with 5% BSA in Tris-buffered saline containing 0.5% Tween-20 (TBST) for 60 min, and then incubated overnight at 4°C with the following primary antibodies: KIF15 antibody (1:1000; cat. no. FNab04551; Fine Test), cyclin D1(CCND1) antibody (1:2,000; cat. no. ab134175; Abcam), cyclin-dependent kinase 6(CDK6) antibody (1:1,000; cat. no. ab151247; Abcam), mitogen-activated protein kinase 9(MAPK9) antibody (1:3,000; cat. no. ab76125; Abcam), phosphatidylinositol-4,5-bisphosphate 3-kinase, catalytic subunit alpha (PIK3CA) antibody (1:1,000; cat. no. ab40776; Abcam), and GAPDH (1:3,000; cat. no. AP0063; Bioworld). Following three times of washing with TBST for 5 min, the membranes were incubated with HRP-conjugated goat anti-rabbit IgG polyclonal secondary antibody (1:3,000; cat. no. A0208; Beyotime) for 1 h. Immobilon Western Chemiluminescent HRP Substrote (cat. no. RPN2232; Millipore) was used for developing color. Each membrane was visualized using the ECL-Plus™ Western blotting system (AI600 ,GE), and detected with an X-ray imaging analyzer. Densitometric analysis was performed using ImageJ (version 1.8.0; National Institutes of Health).

RNA interference and transfection

The BR-V-108 carrier was used in this study. Three specific short hairpin RNAs (siRNAs) against KIF15 (siKIF15-1, siKIF15-2 and siKIF15-3) and a negative control siRNA (shCtrl) were packaged and purchased from GenePharma Co., Ltd., Shanghai, China. Lipofectamine 3000 transfection reagent (Invitrogen, Carlsbad, CA, USA) was used in accordance with the specifications. The sequences of siKIFs were as follows: shKIF15-1 (GCT GAA GTG AAG AGG CTC AAA); shKIF15-2 (AGG CAG CTA GAA TTG GAA TCA); shKIF15-3 (AAG CTC AGA AAG AGC CAT GTT). C666-1 cells were infected with 40 μl of lentivirus at a

concentration of 1×10^8 TU/ml,while CNE-2Z cells were infected with 20 μl according MOI(Multiplicity of Infection). After the transduction into cells, puromycin was added to culture medium to enrich the stably infected cells. The transfection and knockdown efficiencies were verified by light microscopy, fluorescence microscope, qRT-PCR and Western blot.

MTT assay

3-(4,5-Dimethylthiazol-2-yl)-2,5-diphenyltetrazolium bromide (MTT assay was applied to analyze cell viability *in vitro*. C666-1 and CNE-2Z cells were placed into 96-well plates with a density of 1500 cells/well, and cultured for 5 days. MTT solution (20 μl/well, 5 mg/ml) was added to plates. After another 4 h of incubation, Dimethyl Sulphoxide (DMSO ,100 μl/well) was added to dissolve the formazan crystals. Finally, after oscillated for 2–5 min, the absorbance values were measured at 490 nm using a microplate reader (cat. no. M2009PR; Tecan infinite) after 24 h, 48 h, 72 h, 96 h, and 120 h of growth.

Apoptotic assay

Both shKIF15 cells and shCtrl cells were seeded in 6-well plates. The cells were subsequently digested with trypsin, centrifuged at 1300 rpm for 5 min, and washed with D-Hanks at 4°C. Cells were resuspended by binding buffer (200 μl), then Annexin V- APC(10 μl)was used to stain the cells for 15 min in dark at room temperature. Flow cytometer (Millipore, USA) was used to analyzed the Annexin V-APC of the stained cells,which showed red fluorescence. Each experiment was performed in triplicate. The results were visualized by using GuavaSoft software.

Colony formation assay

For colony formation assay, cells were seeded in 6-well plates at a density of 1,000 cells per well and grown for 2 weeks. The culture medium was replaced every 3 days. After that, cells were fixed with 4% paraformaldehyde (1ml/well) and followed by Giemsa staining (500 μl/well) for 20 min. Then, cells were washed with dd H_2O several times. Finally, photographs were taken, and the colonies were counted. Each experiment was performed in triplicate.

Wound healing

The cell suspension was added to a 96-well plate at a concentration of 5×10^4 cells per well. Cells were cultured for a day in serum-free medium, and then wounds were generated by pipette tips. The medium was refreshed with DMEM, and the distance of wound healing was separately observed at 0 h, 24 h and 48 h after wound generation. The cell migration rate of each group was calculated according to the measurement of the width of the wound.

Cell migration assay

Transwell chambers (Corning, cat.no. 3422, USA) were used for cell migration assays. 50,000 NPC cells maintained in 100 μl serum-free medium were seeded into the upper compartment and 600 μl medium supplemented with 30% FBS was added to the bottom compartment. After incubation for 48 h at 37°C, cells remaining in the top were removed by cotton swabs, while cells migrating to the bottom were

stained with 0.1% crystal violet (400μl/well) for 5 min. The migrated cells were photographed and counted under microscope. Cell migration was determined by observing 5 random fields under microscope.

Tumor-bearing mouse model and in vivo **imaging assay**

All the animal experimental protocols were approved by the Ethics committee at People's Hospital of Guangxi Zhuang Autonomous Region. Both shCtrl and shKIF15 group were consisted of 10 BALB/c male nude mice (4 weeks old). They were cultured in the laboratory with a 12 h day/night environment and fed with a standard diet. C666-1 cells, transfected with shKIF15 or shCtrl, 200μl of cell suspension was injected subcutaneously into the back next to the right forelimb of the nude mice at a concentration of 2×10^7 cells/ml. The tumor growth was observed from the fifth day after injection. Then tumors were measured every 4 day until the eighteenth day post-injection. Before the mice were sacrificed, vivisection imager system (Perkin Elmer, Massachusetts, USA) was used for in vivo imaging, and quantitative analysis of fluorescence intensity was performed. All mice were sacrificed by injecting 1% pentobarbital sodium before reaching the humane endpoint. Subcutaneous tumor tissues were harvested, weighted and used for immunohistochemistry (IHC) analysis and hematoxylin eosin (HE) staining.

Protein array analysis

ShKIF15 and shCtrl C666-1 cells were used in the protein array analysis facilitated by human apoptosis antibody array (ab134001, Abcam, UK), according to the manufacturer's instructions. The intensity scores of each array point by were assessed ImageJ software. The expression levels of apoptosis-related proteins in shKIF15 group and shCtrl group were compared.

Statistical analysis

All experiments were carried out in at least 3 independent experiments. Data were expressed as the mean ± standard deviation for continuous analysis. The statistical analyses were carried out using the software of GraphPad Prism version 6. The Student’s t test and $\chi 2$ test were used to analyze significant difference between two groups. Age groups were divided by the median age of all patients. Mann-Whitney U test and Spearman rank correlation analysis were used in the analysis of the relevant data of tissue chips. Kaplan-Meier survival analysis and log-rank test were used for the survival analysis. $P < 0.05$ was considered to indicate a statistically significant difference.

Results

KIF15 was highly expressed in NPC tissues and significantly correlated with poor patient survival

The gene expression profiling data collected from GEO database was examined to preliminarily investigate the role of KIF15 in NPC. The results showed that KIF15 mRNA expression level in

nasopharyngeal carcinoma tissues was significantly higher than normal samples (Fig. 1a-c, logFC = 1.637 and P = 2.5E-06).

In order to clarify the protein expression of KIF15 in nasopharyngeal carcinoma tissue, 132 samples of NPC tissue were applied for IHC analysis. Notably, a total of 17 cases could not be scored because of tissue peeling or poor staining quality. According to the analysis, the protein expression of KIF15 in NPC tissues was significantly higher than that in para-carcinoma tissues (Table 1 and Fig. 1f).

Table 1. Expression patterns in nasopharyngeal carcinoma tissues and para-carcinoma tissues revealed in immunohistochemistry analysis.

KIF15 expression	Tumor tissue		Para-carcinoma tissue		p value
	Cases	Percentage	Cases	Percentage	
Low	60	52.20%	15	100%	0.000***
High	55	47.80%	0	-	

High and low expression were distinguished by the KIF15 expression. ***,P□0.001;

Subsequently, it was found that the protein expression of KIF15 was related to the clinical stage and recurrence, but not to age, gender, tumor size, and lymph node metastasis (Table 2). Spearman rank correlation analysis showed that the expression of KIF15 is positively correlated with clinical staging (P = 0.002, two-tailed). In other words, as the malignant degree of the patient's tumor deepens, the expression of KIF15 protein increases, vice versa. Moreover, according to Kaplan-Meier survival analysis, the expression of KIF15 is significantly related to overall survival (OS, Fig. 1d) and progression-free survival (PFS, Fig. 1e) of nasopharyngeal carcinoma. These results suggested that increased KIF15 expression is a potential indicator of worse clinical outcome of patients with NPC.

Table 2. Relationship between KIF15 expression and tumor characteristics in patients with nasopharyngeal carcinoma.

Features	No. of patients	KIF15 expression		p value
		low	high	
All patients	115	59	56	
Age (years)				0.226
≤47	58	33	25	
> 47	57	26	31	
Gender				0.533
Male	87	46	41	
Female	28	13	15	
Tumor size#				0.53
< 1.2cm	47	26	21	
≥1.2cm	55	27	28	
Stage				0.002**
1	15	8	7	
2	52	35	17	
3	33	14	19	
4	15	2	13	
Recurrence				0.020*
no	62	38	24	
yes	53	21	32	
Cervical lymph node metastasis				0.986
no	35	18	17	
yes	80	41	39	

Some patients' clinical data were not available. *,P□0.05;**□P□0.01.

Construction of KIF15 knockdown cell models

In order to clarify the role of KIF15 in nasopharyngeal carcinoma, we first performed qRT-PCR detection on cell lines commonly used in NPC research. It was found that the 5-8F line possessed significantly lower KIF15 expression than other three cell lines (CNE-2Z, C666-1, HONE-1, shown in Fig. 2a). Moreover, shKIF15-1 RNAi sequence was identified as the most efficient sequence for KIF15 knockdown (Fig. 2b). Then cell lines C666-1 and CNE-2Z were selected for the construction of KIF15-knockdown cell models. The cells transfected with the corresponding empty vector were used as the negative control (shCtrl). Over 80% transduction efficiency in both c666-1 and CNE-2Z cells was observed by detecting the fluorescence of green fluorescent protein (GFP) on lentivirus vector (Fig. 2c). Successful knockdown of KIF15 in shKIF15 group was verified by qPCR (Fig. 2d, upper) and WB (Fig. 2d, lower). In summary, the shKIF15 and shCtrl cell models were successfully constructed for the following studies.

KIF15 knockdown regulated proliferation, apoptosis of NPC cellsin vitro

In order to find out whether the knockdown of KIF15 affects the biological behavior of nasopharyngeal cancer cells such as proliferation and apoptosis, a series of *in vitro* experiments were subsequently

carried out. The results of MTT assay showed that, compared with the shCtrl group, the cell proliferation of the shKIF15 group was significantly inhibited in C666-1 and CNE-2Z. In terms of cell apoptosis, it was demonstrated that the number of apoptotic cells in the shKIF15 group increased significantly after lentivirus infection (shown in Fig. 2e). These findings indicated that the expression of KIF15 in nasopharyngeal carcinoma cells may promote tumor cell proliferation and reduce cell apoptosis.

Up-regulating the expression of KIF15 enhances the clonogenic and migration abilities of NPC cells

Next, we investigated the changes in colony formation and migration ability (an important indicator of tumor metastasis) of nasopharyngeal carcinoma cells induced by KIF15 knockdown. The results of the clone formation assay showed that after KIF15 knockdown, the number of clones in the shKIF15 group was significantly reduced compared to the shCtrl group for both C666-1 ($P < 0.001$, fold change = -2.9, upper part of the Fig. 3a) and CNE2Z ($P < 0.001$, fold change = -4.8, lower part of the Fig. 3a) cell lines. In the following wound healing and transwell assays, the shCtrl group showed its advantages in migration capabilities. In wound healing assay, compared with the shCtrl group, the C666-1 cell migration rate of the shKIF15 group was reduced by 29% at 48 h ($P < 0.001$, Fig. 3b left), and the same index of CNE2Z cells was 8% ($P < 0.05$, Fig. 3b right). Transwell assay showed that the migration rate of shKIF15 group was reduced by 66.7% (C666-1) and 72.6% (CNE2Z) comparing with shCtrl group (Fig. 3c), respectively.

Suppression of KIF15 inhibits tumor progression in vivo

The influence of KIF15 depletions on NPC tumor growth *in vivo* was investigated in this part. Mice xenograft models were established based on nude mice through subcutaneous injection of C666-1 cells treated with shKIF15 or shCtrl. Eighteen days after injection, all mice in the shCtrl group formed tumors under the skin, while only four mice in the shKIF15 group (Fig. 4b). Fluorescence intensity (Fig. 4a), Tumor volume (Fig. 4c), and tumor weight (Fig. 4d) were evaluated as the representation of tumor development, all of which indicated that down-regulation expression of KIF15 could inhibit the development of NPC in mice. After the mice were sacrificed, the sections of xenografts were processed for HE and Ki-67 staining. The immunohistochemistry data showed that Ki-67 expression, which is a biomarker of tumor growth, was much higher in shCtrl group (Fig. 4e). Collectively, knockdown of KIF15 was capable of inhibiting tumor development of NPC *in vivo*.

Mechanistic study of KIF15 in apoptosis pathway

In order to explore the potential mechanism of KIF15 induced regulation of cell apoptosis in NPC. A Human Apoptosis Antibody Array kit, which includes 43 human apoptosis related proteins, was used to identify differentially expressed proteins in shCtrl and shKIF15 C666-1 cells. As a result, we found that the expression levels of HSP27(heat shock 27kDa protein 1), HSP60(heat shock 60kDa protein 1), HSP70(heat shock 70kDa protein 1A), IGF-I (insulin-like growth factor-I), IGF-II (insulin-like growth factor-II), IGFBP-2 (insulin-like growth factor-binding protein-2), IGF-1sR (insulin-like growth factor-1 receptor), and sTNF-R1 (Soluble tumor necrosis factor receptor 1) were significantly down-regulated in KIF15

knockdown group ($P < 0.05$, shown in Fig. 5a-5c). These results suggested that KIF15 could inhibit apoptosis of NPC cells through regulating the expression of the above apoptotic proteins. Moreover, the effects of KIF15 on the activation of the PI3K-AKT signal pathway were also investigated based on the detection of CCND1, CDK6, MAPK9, PIK3CA by western blot analysis. The results indicated that, the expression of CCND1, CDK6 and PIK3CA was downregulated, whereas the expression of MAPK9 was upregulated, indicating the inhibition of the PI3K-AKT signal pathway by KIF15 knockdown (Fig. 5d).

Discussion

KIFs are composed of two heavy chains and two light chains. Their heads are a highly conserved motion domain, which can hydrolyze ATP and conduct chemical energy along microtubules to promote mechanical movement. In contrast, the tails are combined with a specific cargo through a light chain, and the cargo may include vesicles, organelles or macromolecules [15]. More importantly, KIFs can also participate in chromosome congression, alignment and cytokinesis [6, 16]. They are strictly regulated through temporal synthesis and only present when needed[17, 18]. However, the dysregulation of KIFs may lead to uncontrolled cell growth in the development of many types of human cancers [19]. For example, the overexpression of mitotic kinesins may lead to an imbalance of outward movement, leading to a series of excessive spindle separation, and ultimately unequal distribution of DNA leading to aneuploidy [20]. On the contrary, the down-regulation of some kinesins leads to mitotic arrest and failure of cytokinesis, thereby stimulating the apoptotic pathway and even leading to primary microcephaly and Braddock-Carey Syndrome (BCS) [21]. Therefore, better understanding of functions of kinesin proteins may contribute to the development of targeted therapy for cancers.

In this study, nasopharyngeal carcinoma was found to have high mRNA expression of KIF15 by bioinformatics analysis. The protein expression of KIF15 in NPC tissues was significantly higher than para-carcinoma tissues, which was significantly correlated with cancer grades, recurrence and predicted a poor prognosis of patients. Similar results have also been reported in hepatocellular carcinoma [10], lung cancer [12], breast cancer [22] and other tumors [13, 23]. All these indicate that the high expression of KIF15 is an unfavorable factor for the prognosis of tumor patients.

Based on the clinical findings described above, we hypothesized that overexpression of KIF15 in NPC may promote cancer progression. Therefore, C666-1 and CNE-2Z cell lines were selected to construct KIF15 knockdown cell models for loss-of-function study *in vitro*. The results revealed that the silencing of KIF15 inhibited cell proliferation and induced cell apoptosis. Moreover, we further found that knocking down KIF15 can significantly inhibit cell motility of NPC, which is of great significance to tumor progression and metastasis, and also explains that patients with high expression of KIF15 suffer from a higher risk of recurrence from another perspective. As expected, both *in vitro* colony formation assay and *in vivo* xenograft assay showed that the tumor formation ability of shKIF15 cells was suppressed, which further lead to slower growth of xenografts. These findings suggest that the high expression of KIF15 in nasopharyngeal carcinoma cells can promote proliferation and migration, reduce apoptosis and enhance tumorigenic ability.

Apoptosis is a process that occurs in multicellular when a cell intentionally "decides" to die [24]. Once the apoptosis program is started, various apoptosis-related proteins in the cell gather together and then enter the continuous reaction process. Previous studies have confirmed that KIFs also play an important role in apoptosis [14, 19, 25], therefore, we focus on the change of apoptosis in NPC cells after KIF15 knockdown and the underlying mechanisms. We provided biological evidence that HSP27, HSP60, HSP70, IGF-I, IGF-II, IGFBP-2, IGF-1sR, and sTNF-R1 were significantly down-regulated in KIF15 knockdown NPC cells. HSP27, HSP60, HSP70 have protective effects on cell apoptosis caused by heat shock stress, oxidative stress and ionizing radiation [26]. sTNF-R1 is a soluble form of TNFR. It is generally believed that sTNF-R1 possesses the ability to limit TNF activity, or stabilize TNF, and has an important regulatory role in the cytokine network [27]. Given that IGF-I, IGF-II, IGFBP-2, IGF-1sR are members of the insulin-like growth factor system, which could inhibit apoptosis by activating the PI3K/AKT pathway [28], we implied that KIF15 might induce the suppression of apoptosis in NPC via the PI3K/AKT pathway. Subsequent results of western blot analysis confirmed that multiple signaling pathways, including PI3K/AKT (activation) and MAPK (de-activation) signaling pathways, may be involved in the promotion of the development of nasopharyngeal carcinoma by KIF15. However, the molecular mechanism of KIF15 is still unclear, and further studies will be required in NPC.

Induction and adjuvant chemotherapy is an essential part of the treatment in NPC patients [2, 29]. Docetaxel and paclitaxel, as a class of anti-microtubule taxane, are often used in the first- or second-line treatment of nasopharyngeal carcinoma. Unfortunately, resistance to chemotherapy remains a critical medical challenge, and many KIFs are associated with resistance to docetaxel and paclitaxel [30–33]. Therefore, it is a meaningful attempt to develop targeted drugs for KIFs. On the one hand, it can inhibit the biological characteristics of cancer cell proliferation and infiltration; on the other hand, it may reduce the occurrence of drug resistance and improve the therapeutic effect of NPC patients. One promising target is KIF11 (Eg5), a kinesin that plays a key role in spindle formation by generating forces that separate the two poles. But in a Phase I trial, Eg5 inhibitors are less effective than expected when cancer cells develop resistance to them by escalating the expression of KIF15 as alternative to Eg5[34–36]. Therefore, the drugs that target KIF15 may be used in combination with Eg5 inhibitors [37, 38], which provides an interesting idea for us to develop similar drugs for treating nasopharyngeal carcinoma in the future.

Conclusion

In conclusion, we demonstrated that KIF15 is overexpressed and accelerated the progression of nasopharyngeal carcinoma. It can be used as a new prognostic indicator as well as a potential therapeutic target for the treatment of NPC.

Declarations

Acknowledgements

None.

Authors' contributions

GWH designed the research. YLW took part in designing the research, performed the experiments, analyzed the date and wrote the manuscript. YY, FL took part in the experiments. YLW and YQ collected the data. JCS and BL participated in the process of analyzing the date. SHQ provided technical assistance during the experiment. All authors read and approved the final manuscript.

Funding

This work was supported by Guangxi Key Research and Development Plan (Guangxi Branch AB18050011).

Availability of data and materials

Please contact author for data requests.

Ethics approval and consent to participate

The tissue microarray protocol was approved by the Human Ethics Committee of the Taizhou Hospital of Zhejiang province. Date of adoption: January 26, 2010; Certificate No.: 2010.2.8.

The animal experimental protocols were approved by the Ethics Committee of the People's Hospital of Guangxi Zhuang Autonomous Region; Date of adoption: August 21, 2018; Certificate No.: Research-2018-47.

Consent for publication

Not applicable.

Competing interests

The authors report no competing interest in this study.

References

1. Tao Q, Chan AT. Nasopharyngeal carcinoma: molecular pathogenesis and therapeutic developments. Expert Rev Mol Med. 2007;9(12):1–24.
2. Lee AWM, Tung SY, Ng WT, Lee V, Ngan RKC, Choi HCW, Chan LLK, Siu LL, Ng AWY, Leung TW, et al. A multicenter, phase 3, randomized trial of concurrent chemoradiotherapy plus adjuvant chemotherapy versus radiotherapy alone in patients with regionally advanced nasopharyngeal carcinoma: 10-year outcomes for efficacy and toxicity. Cancer. 2017;123(21):4147–57.

3. Chen L, Hu CS, Chen XZ, Hu GQ, Cheng ZB, Sun Y, Li WX, Chen YY, Xie FY, Liang SB, et al. Concurrent chemoradiotherapy plus adjuvant chemotherapy versus concurrent chemoradiotherapy alone in patients with locoregionally advanced nasopharyngeal carcinoma: a phase 3 multicentre randomised controlled trial. The Lancet Oncology. 2012;13(2):163–71.
4. Logan CM, Menko AS. Microtubules: Evolving roles and critical cellular interactions. Experimental biology medicine. 2019;244(15):1240–54.
5. Ong MS, Deng S, Halim CE, Cai W, Tan TZ, Huang RY, Sethi G, Hooi SC, Kumar AP, Yap CT. **Cytoskeletal Proteins in Cancer and Intracellular Stress: A Therapeutic Perspective**. *Cancers* 2020, 12(1).
6. Vanneste D, Ferreira V, Vernos I. Chromokinesins: localization-dependent functions and regulation during cell division. Biochemical Society transactions. 2011;39(5):1154–60.
7. Zou JX, Duan Z, Wang J, Sokolov A, Xu J, Chen CZ, Li JJ, Chen HW. Kinesin family deregulation coordinated by bromodomain protein ANCCA and histone methyltransferase MLL for breast cancer cell growth, survival, and tamoxifen resistance. Molecular cancer research: MCR. 2014;12(4):539–49.
8. Gao X, Zhu L, Lu X, Wang Y, Li R, Jiang G. **KIF15 contributes to cell proliferation and migration in breast cancer**. *Human cell* 2020.
9. Wang J, Guo X, Xie C, Jiang J. KIF15 promotes pancreatic cancer proliferation via the MEK-ERK signalling pathway. British journal of cancer. 2017;117(2):245–55.
10. Kitagawa A, Masuda T, Takahashi J, Tobo T, Noda M, Kuroda Y, Hu Q, Kouyama Y, Kobayashi Y, Kuramitsu S, et al. KIF15 Expression in Tumor-associated Monocytes Is a Prognostic Biomarker in Hepatocellular Carcinoma. Cancer genomics proteomics. 2020;17(2):141–9.
11. Matsushita J, Suzuki T, Okamura K, Ichihara G, Nohara K. Identification by TCGA database search of five genes that are aberrantly expressed and involved in hepatocellular carcinoma potentially via DNA methylation changes. Environ Health Prev Med. 2020;25(1):31.
12. Qiao Y, Chen J, Ma C, Liu Y, Li P, Wang Y, Hou L, Liu Z. Increased KIF15 Expression Predicts a Poor Prognosis in Patients with Lung Adenocarcinoma. Cellular physiology biochemistry: international journal of experimental cellular physiology biochemistry pharmacology. 2018;51(1):1–10.
13. Ding L, Li B, Yu X, Li Z, Li X, Dang S, Lv Q, Wei J, Sun H, Chen H, et al. KIF15 facilitates gastric cancer via enhancing proliferation, inhibiting apoptosis, and predict poor prognosis. Cancer cell international. 2020;20:125.
14. Terribas E, Fernandez M, Mazuelas H, Fernandez-Rodriguez J, Biayna J, Blanco I, Bernal G, Ramos-Oliver I, Thomas C, Guha R, et al. KIF11 and KIF15 mitotic kinesins are potential therapeutic vulnerabilities for malignant peripheral nerve sheath tumors. Neuro-oncology advances. 2020;2(Suppl 1):i62–74.
15. Boleti H, Karsenti E, Vernos I. Xklp2, a novel Xenopus centrosomal kinesin-like protein required for centrosome separation during mitosis. Cell. 1996;84(1):49–59.
16. Wittmann T, Boleti H, Antony C, Karsenti E, Vernos I. Localization of the kinesin-like protein Xklp2 to spindle poles requires a leucine zipper, a microtubule-associated protein, and dynein. J Cell Biol.

1998;143(3):673–85.
17. Gruneberg U, Neef R, Honda R, Nigg EA, Barr FA. Relocation of Aurora B from centromeres to the central spindle at the metaphase to anaphase transition requires MKlp2. J Cell Biol. 2004;166(2):167–72.
18. Vanneste D, Takagi M, Imamoto N, Vernos I. The role of Hklp2 in the stabilization and maintenance of spindle bipolarity. Current biology: CB. 2009;19(20):1712–7.
19. Li Q, Qiu J, Yang H, Sun G, Hu Y, Zhu D, Deng Z, Wang X, Tang J, Jiang R. Kinesin family member 15 promotes cancer stem cell phenotype and malignancy via reactive oxygen species imbalance in hepatocellular carcinoma. Cancer letters. 2020;482:112–25.
20. Lucanus AJ, Yip GW. Kinesin superfamily: roles in breast cancer, patient prognosis and therapeutics. Oncogene. 2018;37(7):833–8.
21. Sleiman PMA, March M, Nguyen K, Tian L, Pellegrino R, Hou C, Dridi W, Sager M, Housawi YH, Hakonarson H. Loss-of-Function Mutations in KIF15 Underlying a Braddock-Carey Genocopy. Hum Mutat. 2017;38(5):507–10.
22. Zeng H, Li T, Zhai D, Bi J, Kuang X, Lu S, Shan Z, Lin Y. ZNF367-induced transcriptional activation of KIF15 accelerates the progression of breast cancer. Int J Biol Sci. 2020;16(12):2084–93.
23. Wang Q, Han B, Huang W, Qi C, Liu F. Identification of KIF15 as a potential therapeutic target and prognostic factor for glioma. Oncol Rep. 2020;43(4):1035–44.
24. Elmore S. Apoptosis: a review of programmed cell death. Toxicol Pathol. 2007;35(4):495–516.
25. Castillo A, Morse HC 3rd, Godfrey VL, Naeem R, Justice MJ. Overexpression of Eg5 causes genomic instability and tumor formation in mice. Cancer research. 2007;67(21):10138–47.
26. Kennedy D, Jager R, Mosser DD, Samali A. Regulation of apoptosis by heat shock proteins. IUBMB Life. 2014;66(5):327–38.
27. Vielhauer V, Mayadas TN. Functions of TNF and its receptors in renal disease: distinct roles in inflammatory tissue injury and immune regulation. Semin Nephrol. 2007;27(3):286–308.
28. Malaguarnera R, Belfiore A. The emerging role of insulin and insulin-like growth factor signaling in cancer stem cells. Front Endocrinol. 2014;5:10.
29. Zhang Y, Chen L, Hu GQ, Zhang N, Zhu XD, Yang KY, Jin F, Shi M, Chen YP, Hu WH, et al. Gemcitabine and Cisplatin Induction Chemotherapy in Nasopharyngeal Carcinoma. N Engl J Med. 2019;381(12):1124–35.
30. Singel SM, Cornelius C, Batten K, Fasciani G, Wright WE, Lum L, Shay JW. A targeted RNAi screen of the breast cancer genome identifies KIF14 and TLN1 as genes that modulate docetaxel chemosensitivity in triple-negative breast cancer. Clinical cancer research: an official journal of the American Association for Cancer Research. 2013;19(8):2061–70.
31. Lee J, Cho YJ, Lee JW, Ahn HJ. KSP siRNA/paclitaxel-loaded PEGylated cationic liposomes for overcoming resistance to KSP inhibitors: Synergistic antitumor effects in drug-resistant ovarian

cancer. Journal of controlled release: official journal of the Controlled Release Society. 2020;321:184–97.

32. Ganguly A, Yang H, Cabral F. Overexpression of mitotic centromere-associated Kinesin stimulates microtubule detachment and confers resistance to paclitaxel. Mol Cancer Ther. 2011;10(6):929–37.
33. Khongkow P, Gomes AR, Gong C, Man EP, Tsang JW, Zhao F, Monteiro LJ, Coombes RC, Medema RH, Khoo US, et al. Paclitaxel targets FOXM1 to regulate KIF20A in mitotic catastrophe and breast cancer paclitaxel resistance. Oncogene. 2016;35(8):990–1002.
34. Gomez HL, Philco M, Pimentel P, Kiyan M, Monsalvo ML, Conlan MG, Saikali KG, Chen MM, Seroogy JJ, Wolff AA, et al. Phase I dose-escalation and pharmacokinetic study of ispinesib, a kinesin spindle protein inhibitor, administered on days 1 and 15 of a 28-day schedule in patients with no prior treatment for advanced breast cancer. Anti-cancer drugs. 2012;23(3):335–41.
35. Groen A. Microtubule motors: a new hope for kinesin-5 inhibitors? Current biology: CB. 2013;23(14):R617–8.
36. Dumas ME, Sturgill EG, Ohi R. Resistance is not futile: Surviving Eg5 inhibition. Cell cycle. 2016;15(21):2845–7.
37. Hancock WO. Mitotic kinesins: a reason to delve into kinesin-12. Current biology: CB. 2014;24(19):R968–70.
38. Sebastian J. Dihydropyrazole and dihydropyrrole structures based design of Kif15 inhibitors as novel therapeutic agents for cancer. Comput Biol Chem. 2017;68:164–74.

Figures

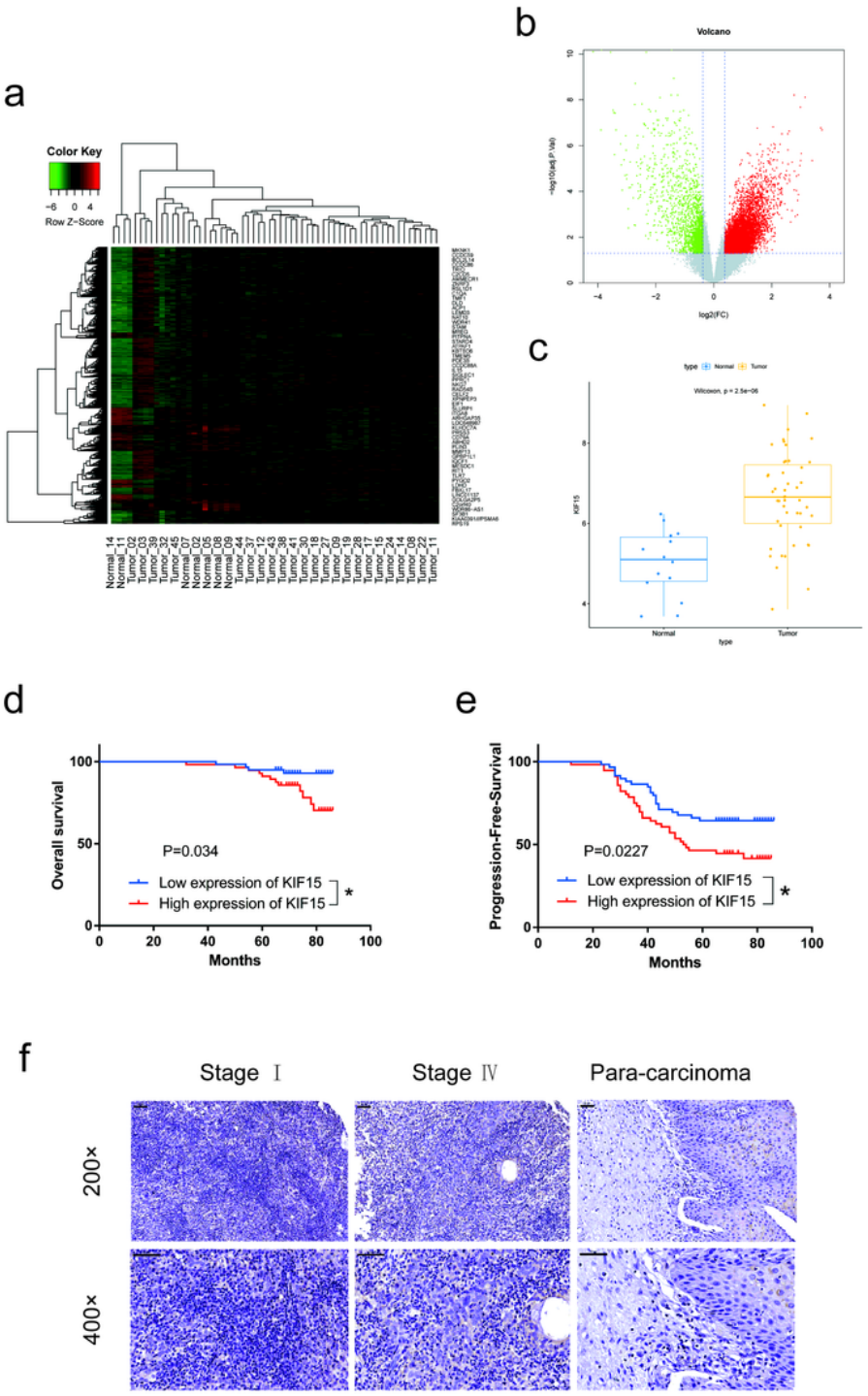

Figure 1

KIF15 was highly expressed in NPC tissues and significantly correlated with poor patient survival. (a) Heat map and (b) Volcano map were used to show genes that have significantly differentially expression of KIF15 in NPC and normal tissues. (c) Box plot showed the expression levels of KIF15 in NPC tissues and normal tissue (logFC=1.6370, P<0.001). (d) Kaplan–Meier survival curves of overall survival (OS, P <

0.05). (e) Kaplan–Meier survival curves of progression-free survival (PFS, P < 0.05). (f) Expression levels of KIF15 in NPC tissues and para-carcinoma tissues were detected by IHC staining, Scale bars: 50 μm.

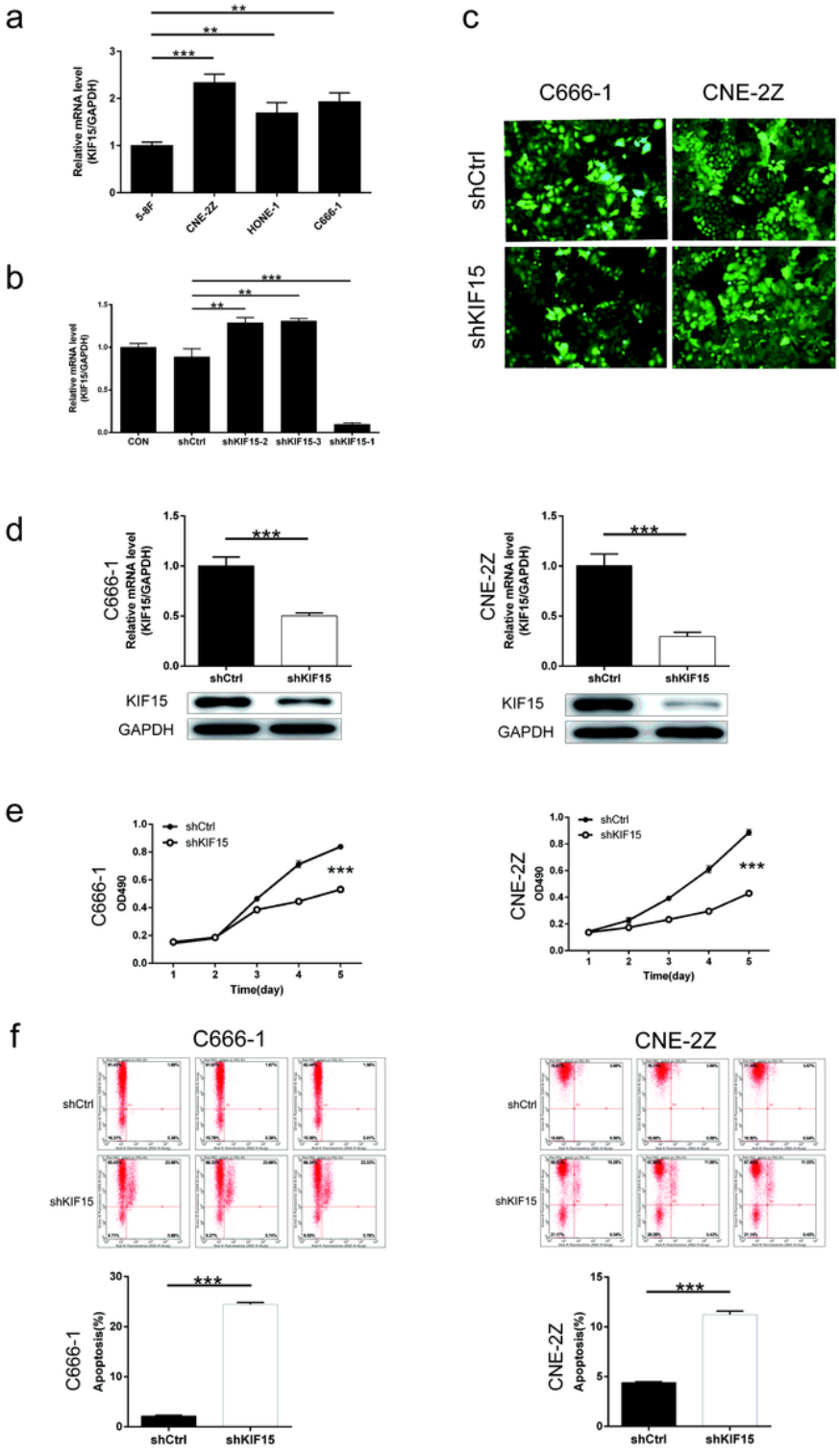

Figure 2

KIF15 knockdown inhibits NPC cell proliferation and induces cell apoptosis in vitro. (a) The background expression of KIF15 in NPC cells was detected by qRT-PCR (P <0.05). (b) Knockdown efficiency of KIF15 by shRNAs (shKIF15-1, shKIF15-2 and shKIF15-3) was examined by qRT-PCR. The knockdown efficiency

of KIF15 in shKIF15-1 group is 89.1% (P<0.001). (c) The fluorescence of cells, which were infected with shCtrl or shKIF15, were observed by microscope to verify the infection efficiency. (d) The knockdown efficiency of KIF15 in NPC cells was detected by qRT-PCR (upper, P<0.001) and Western blot. (e) MTT assay were conducted on C666-1 and CNE-2Z cells with or without KIF15 knockdown to evaluate their proliferation rate (P<0.001). (f) Flow cytometry indicated that C666-1 and CNE-2Z with KIF15 silencing exhibited significantly increased apoptotic rate compared with the control group (P<0.001).

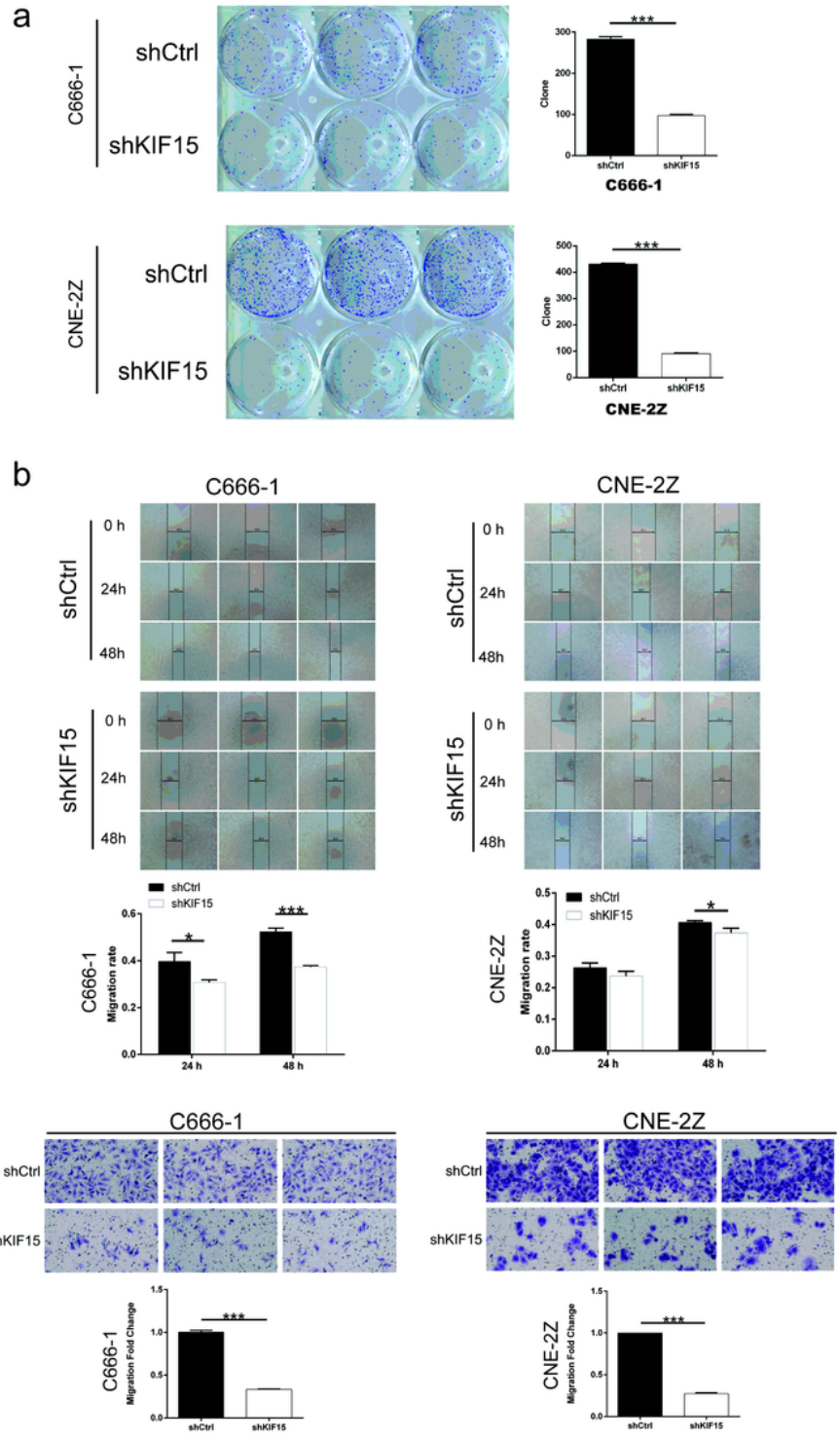

Figure 3

Knockdown of KIF15 inhibits the clonogenic and migration abilities of NPC cells in vitro. (a) The colony formation assay showed that, Cell colony number was significantly decreased in shKIF15 group compared with shCtrl group, both in C666-1 and CNE-2Z cells ($P<0.001$). (b) Wound-healing assay was conducted on the shKIF15 and shCtrl transfected cells to evaluate their migratory ability. In C666-1 cells, the migration rate of cells in shKIF15 group (48 h) was decreased by 29% ($P<0.001$), while in CNE-2Z cells the number was 8% ($P<0.05$). (c) Transwell assay was conducted on transfected cells to evaluate their migration ability: The migration rate of cells in shKIF15 group was decreased by 66.7% ($P<0.001$) in C666-1 cells, and 72.6% ($P<0.001$) in CNE-2Z cells.

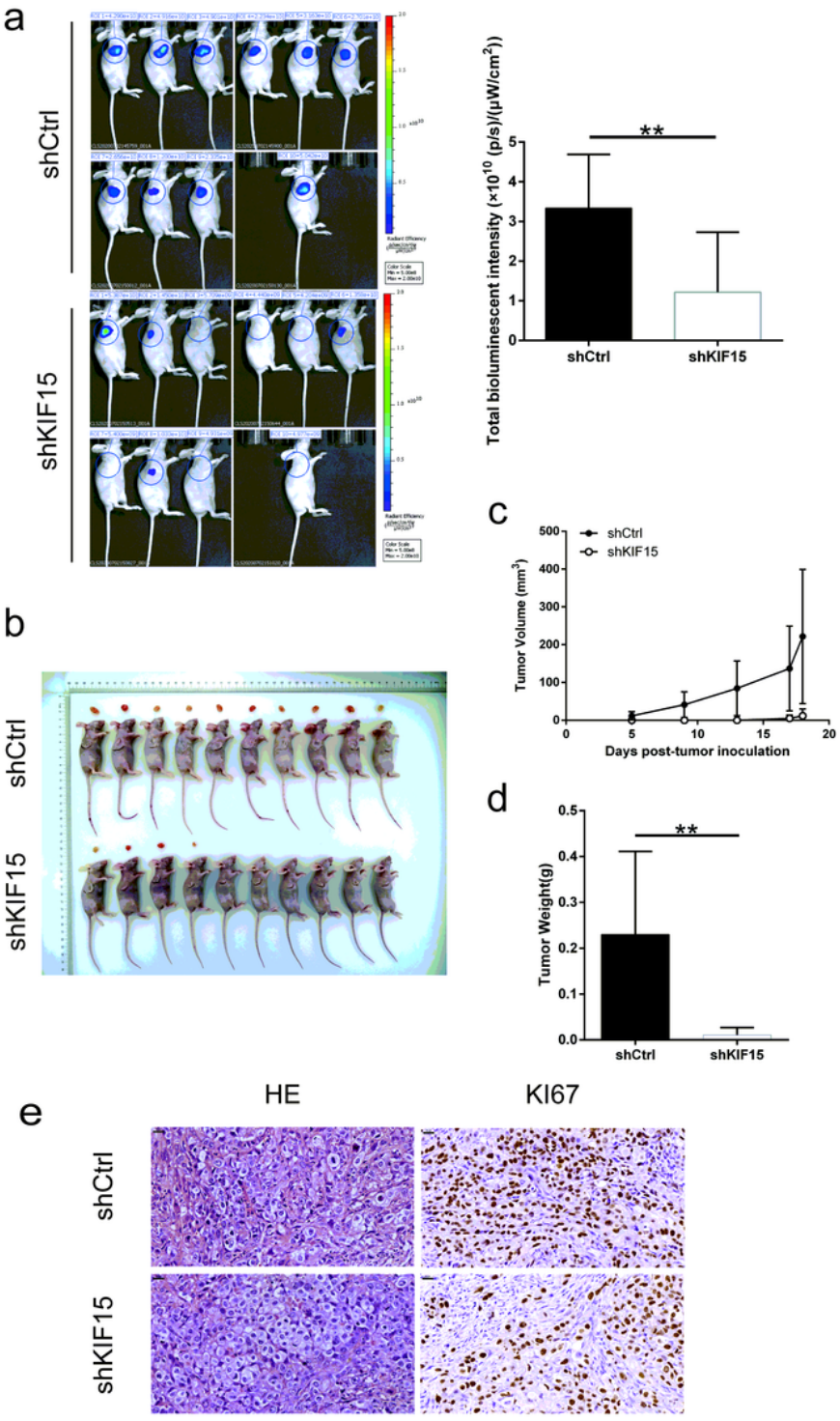

Figure 4

KIF15 silencing repressed NPC tumor progression in vivo. (a) Fluorescence expression was detected in mice, and it was significantly decreased in the shKIF15 group ($P < 0.001$). (b) Eighteen days after injection, all mice in the shCtrl group formed tumors under the skin, while only four mice in the shKIF15 group. (c) Xenogenous tumor volume and (d) weight were assessed, and the results showed that the tumor growth rate slowed down by KIF15 knockdown ($P < 0.001$). (e) The sections of xenografts were

processed for HE and Ki-67 staining. Under the microscope of 200 times, Ki-67 staining was reduced in shKIF15 group compared with shCtrl group, Scale bars: 20 μm.

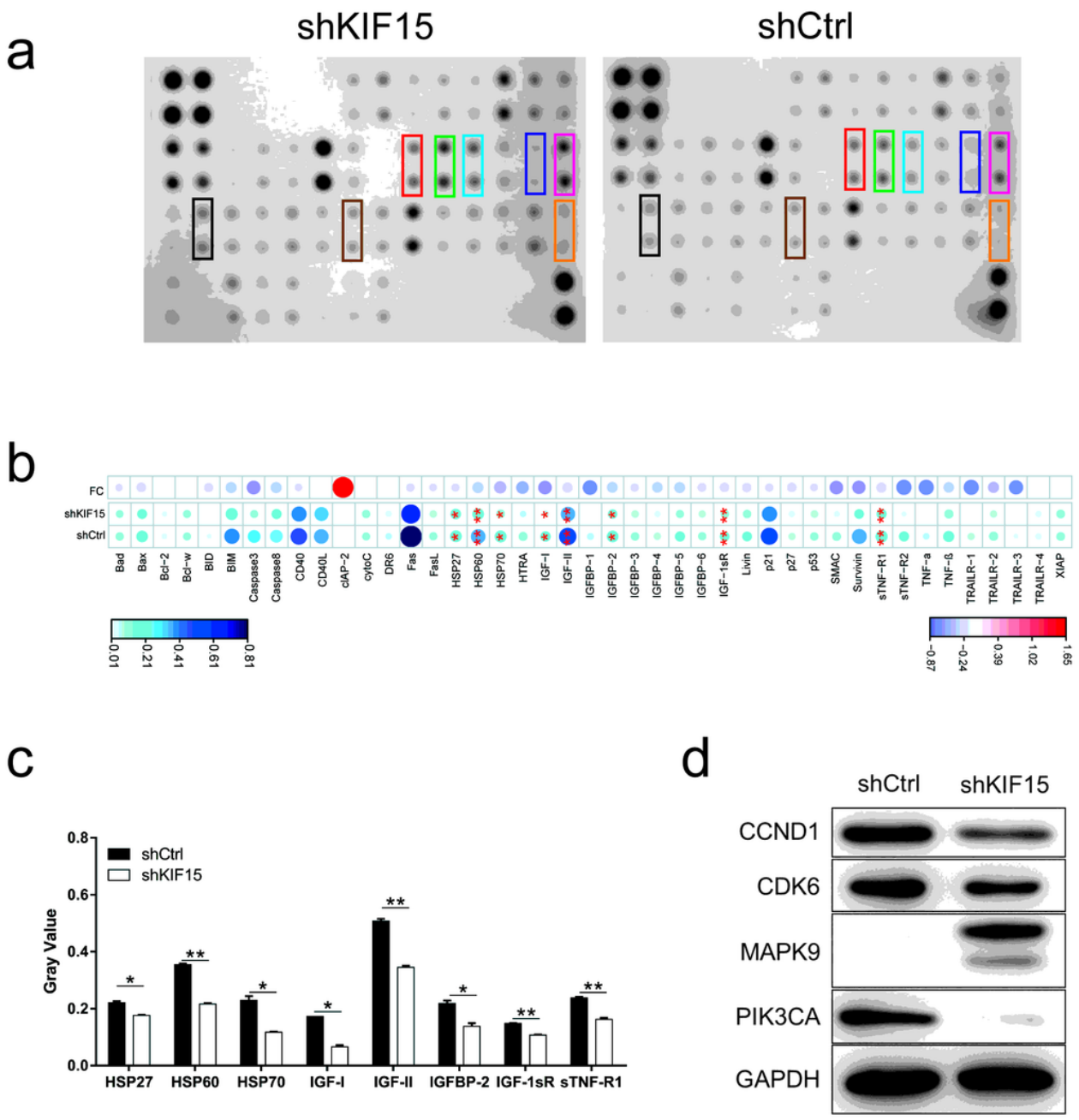

Figure 5

Knockdown of KIF15 decreases expression of seven apoptotic proteins in NPC. (a) Human apoptosis antibody array analysis was performed in shCtrl and shKIF15 C666-1 cells. (b) Grayscale results and analysis of human apoptosis antibody array. (c) The results showed that the expression levels of seven apoptosis-related proteins decreased significantly in shKIF15 group compared with shCtrl group (*, P <

0.05; **, P < 0.01). (d) The expression levels of CCND1, CDK6, MAPK9, PI3KCA were detected by western blot analysis in shCtrl and shKIF15 C666-1 cells.